HHS Public Access

Author manuscript

J Cell Sci. Author manuscript; available in PMC 2019 October 23.

Published in final edited form as:

J Cell Sci. 2008 May 01; 121(Pt 9): 1559–1568. doi:10.1242/jcs.021089.

Organellar dynamics during the cell cycle of *Toxoplasma gondii*

Manami Nishi, **Ke Hu**[*], **John M. Murray**, **David S. Roos**[‡]

Departments of Biology, and Cell and Developmental Biology, University of Pennsylvania, Philadelphia PA 19104, USA

Summary

The protozoan phylum Apicomplexa encompasses ~5000 species of obligate intracellular parasites, including those responsible for malaria and toxoplasmosis. Rather than dividing by binary fission, apicomplexans use a remarkable mechanism for replication, assembling daughters de novo within the cytoplasm. Here, we exploit time-lapse microscopy of fluorescent markers targeted to various subcellular structures in *Toxoplasma gondii* tachyzoites to determine how these unicellular eukaryotes efficiently package a complete set of organelles, maintaining the highly polarized organization necessary for host cell invasion and pathogenesis. Golgi division and elongation of the apicoplast are among the first morphologically observable events, associated with an unusual pattern of centriolar migration. Daughter parasites are assembled on cytoskeletal scaffolding, whose growth proceeds from the apical end, first encapsulating the divided Golgi. Further extension of the cytoskeletal scaffold results in partitioning of the apicoplast, nucleus, endoplasmic reticulum, and finally the mitochondrion, which enters the developing daughters rapidly, but only very late during the division cycle. The specialized secretory organelles (micronemes and rhoptries) form de novo. This distinctive pattern of replication – in which organellar segregation spans ~75% of the cell cycle, completely encompassing S phase – suggests an unusual mechanism of cell cycle regulation.

Keywords

Apicomplexan parasites; Organelle segregation; Apicoplast; Mitochondrion; Endoplasmic reticulum; Golgi; Centrioles; Micronemes; Rhoptries

Introduction

The apicomplexan parasite cell (Fig. 1) is enclosed by a pellicle (Nichols and Chiappino, 1987) consisting of a plasma membrane and the inner membrane complex (IMC) – a patchwork of flattened membrane vesicles lying just beneath the plasma membrane and associated with the subpellicular cytoskeleton (Porchet and Torpier, 1977; Dubremetz and Torpier, 1978; Morrissette et al., 1997). An apical complex of specialized cytoskeletal structures and secretory organelles (micronemes and rhoptries) gives the phylum Apicomplexa its name. These secretory organelles, along with dense granules, are thought to

[‡]Author for correspondence (droos@sas.upenn.edu).

[*]Present address: Department of Biology, Indiana University, Bloomington, IN 47405, USA

Supplementary material available online at http://jcs.biologists.org/cgi/content/full/121/9/1559/DC1

be responsible for host-cell recognition, attachment, invasion and establishment/maintenance of the intracellular parasitophorous vacuole (PV), within which replicating parasites reside (Carruthers and Sibley, 1997; Dubremetz et al., 1998). Proteins secreted from rhoptries have recently been shown to play an important role in parasite virulence (Saeij et al., 2006; Taylor et al., 2006; Saeij et al., 2007). Apicomplexan cells also contain a complete set of typical eukaryotic organelles, in a stripped-down form that has facilitated morphological and mechanistic studies (Hager et al., 1999; Joiner and Roos, 2002; Pelletier et al., 2002). Each parasite contains a single interconnected endoplasmic reticulum (ER), one Golgi complex, one nucleus, one mitochondrion and even a plastid acquired by secondary endosymbiosis (Köhler et al., 1997; Roos et al., 1999; Foth and McFadden, 2003).

In contrast to the familiar pattern of cytokinesis typical of animal, plant, fungal and bacterial cells, apicomplexan parasite replication occurs by assembling daughter cells within the mother – a process termed endodyogeny, endopolyogeny or schizongony, depending on the number of daughters formed, and the timing of nuclear division (Sheffield and Melton, 1968; Hu et al., 2002). As daughter cells grow, they encapsulate virtually all of the maternal cell contents, eventually deriving their plasma membrane from that of the mother as they emerge, leaving behind only a small residual body (Sheffield and Melton, 1968). Thus, these parasites must possess a highly coordinated subcellular replication system to ensure that each daughter acquires a complete complement of organelles, maintaining the highly polarized organization required for host cell invasion. Morphological studies on fixed specimens (Ogino and Yoneda, 1966; Sheffield and Melton, 1968; Aikawa, 1971), including three-dimensional reconstructions from serial sections (Slomianny and Prensier, 1986; Bannister et al., 2000a), have helped to define the fine structure of individual organelles, but these approaches are unable to reveal the dynamic process of organellar replication and segregation during cell division.

Fluorescent markers greatly facilitate the study of organellar dynamics in living parasites (Striepen et al., 1998; Striepen et al., 2000; He et al., 2001; Hu et al., 2002; Pelletier et al., 2002; Dzierszinski et al., 2004; Vaishnava et al., 2005; van Dooren et al., 2005; Hartmann et al., 2006; Hu et al., 2006). For example, the parasite Golgi has been shown to elongate laterally before dividing and segregating between the two daughter cells (Pelletier et al., 2002). The apicoplast has been shown to replicate early during endodyogeny, in close synchrony with nuclear division (Striepen et al., 2000; Vaishnava et al., 2005; van Dooren et al., 2005). How do organelles replicate while maintaining highly polarized cell structures? In this study, we have constructed a diverse array of fluorescent markers fused to various organellar proteins or targeting signals. Combining these reporter constructs in various permutations and combinations highlights the dynamic movement and inheritance of organelles from mother to daughter cells during cytokinesis in living *T. gondii* tachyzoites. These studies reveal several unusual aspects of organellar replication, including: early centriolar migration, which appears likely to define the spindle axis; rapid, late entry of the mitochondrion into the developing daughter parasites; and a tightly synchronized process of organellar replication and division during daughter parasite assembly.

Results

During the process of endodyogeny in *Toxoplasma* parasites (and the related, but more complicated process of schizogony in *Plasmodium*) individual organelles must segregate equally between the developing daughter cells, in a spatially and temporally coordinated manner. In order to follow the dynamic processes of organellar replication, we have taken advantage of fluorescent marker proteins to label various subcellular organelles – including the nucleus, ER, Golgi complex, cytoskeletal filaments, mitochondrion and apicoplast – enabling visualization in living parasites by time-lapse microscopy. The inner membrane complex protein IMC1 (Mann and Beckers, 2001; Hu et al., 2002) was used as a marker to precisely track the progress of cytokinesis, because this protein is a component of the subpellicular network that defines the periphery of both the mature parasite tachyzoite and the immature daughters developing with the mother cell.

Previous studies on *T. gondii* and related protists have suggested the following sequence of organellar segregation events during parasite replication: Golgi complex → apicoplast → nucleus (Sheffield and Melton, 1968; Striepen et al., 2000; Pelletier et al., 2002). This pattern was clearly supported by studies on clonal parasite lines stably expressing multiple fluorescent protein reporters or labeled with antibody (Fig. 2). During interphase, the Golgi (GRASP-mRFP; red in Fig. 2, left column), apicoplast [anti-acyl carrier protein (ACP); red in Fig. 2, middle and right columns] and centrioles [EGFP-*T. gondii* (*Tg*) centrin (Hartmann et al., 2006); green in Fig. 2, right column] were localized in close proximity, near the apical end of the nucleus (Fig. 2A–C). The Golgi underwent elongation (Fig. 2D) and fission (Fig. 2G) before the initiation of daughter scaffold formation [IMC1-YFP (Hu et al., 2002); green in Fig. 2 middle column] (Fig. 2J,K). Elongation of the apicoplast initiated early (Fig. 2E), coincident with centriole migration (Fig. 2F), but apicoplast segregation into daughter parasites (Fig. 2N) took place only after centriole duplication (Fig. 2I) and the initiation of scaffold formation (Fig. 2J,K). Identical results were obtained using various other Golgi and apicoplast reporters (not shown). Karyokinesis followed after fission of the apicoplast (Fig. 2N,O).

The endoplasmic reticulum (ER) forms a network extending from the nuclear envelope (labeled using the ER marker $P30_L$-mRFP-HDEL, red in Fig. 3). At the initiation of daughter scaffold formation (Fig. 3, t=0′), ER entered the daughter scaffolds from the basal side together with the nuclear envelope (white arrowheads) (IMC1-YFP, green). As the IMC scaffold elongates, the ER follows the nucleus, segregating into developing daughters. Apical and basal ramification of the ER continued through karyokinesis (Fig. 3, +90′) and the completion of cell division (Fig. 3, +170′).

Secretion is crucial for the survival of apicomplexan parasites, which use the classical eukaryotic secretory pathway to traffic proteins to the plasma membrane and external environment (Sheffield and Melton, 1968; Joiner and Roos, 2002). Parasite-specific secretory organelles include dense granules (constitutive secretory vesicles), micronemes (regulated secretory organelles involved in host cell attachment and invasion) and rhoptries (regulated secretory organelles involved in establishment and maintenance of the intracellular parasitophorous vacuole) (Carruthers and Sibley, 1997; Joiner and Roos, 2002).

Previous reports have suggested that these organelles may be synthesized de novo, within each daughter cell, during endodyogeny (Ogino and Yoneda, 1966; Sheffield and Melton, 1968; Bannister et al., 2000b). This process could be visualized by time-lapse microscopy of fluorescently labelled parasites, as illustrated in Fig. 4. At the onset of daughter formation (t=0′), maternal micronemes [left two columns, MIC3-GFP (Striepen et al., 1998), green] and rhoptries [right two columns, ROP1-CAT-YFP (Dzierszinski et al., 2004), green] were localized at the apical end of the mother (labeled with IMC1-mRFP, red). As the IMC extends, maternal micronemes and rhoptries remained (+40′, open arrowheads), but new foci along daughter scaffolds also appeared within each daughter (+40′, white arrowheads). The IMC forms a continuous barrier separating the maternal and daughter micronemes and rhoptries, necessitating de novo formation of daughter micronemes and rhoptries, presumably by vesicular budding from the Golgi. Microneme and rhoptry labeling became increasingly distinct as daughter parasites matured (+80–95′, white arrowheads), whereas maternal micronemes and rhoptries (open arrowheads) disappeared, with residual material packaged into the residual bodies (+130–140′).

T. gondii parasites contain a single mitochondrion, typically forming a lasso-shaped structure surrounding the nucleus (Seeber et al., 1998; Melo et al., 2000; Toursel et al., 2000), but the replication of this organelle has not previously been described. To label the *T. gondii* mitochondrion, the N-terminal 55 amino acids from mitochondrial matrix heat shock protein 60 ($HSP60_L$) (Toursel et al., 2000) were fused to the fluorescent protein *Ds*Red and engineered for stable expression in transgenic parasites. Time-lapse microscopy (Fig. 5A) showed that mitochondrial segregation in *T. gondii* is tightly coupled with the cell division cycle [unlike most other eukaryotic systems, where mitochondria replicate autonomously (Bereiter-Hahn and Voth, 1994; Shaw and Nunnari, 2002; Logan, 2006)]. At the onset of daughter IMC formation (t=0′), the mitochondrion formed branches at multiple locations along its length (arrowheads). These extensions continued to grow, ultimately surrounding the growing daughter IMC (Fig. 5A, +60’; corresponds approximately to the bottom row in Fig. 2). Surprisingly, the mitochondrion appeared to be completely excluded from the developing daughters, even very late during scaffold formation, when the daughter parasites began to emerge from the mother (as seen in at least three of the four parasites shown at Fig. 5A, +110′). Mitochondrial branches enter the developing daughters only at the last possible moment, migrating rapidly along the IMC/cytoskeletal scaffolding (Fig. 5A, +120′), and ultimately encircling the nucleus (Fig. 5A, +140′ and supplementary material Movie 1). A small amount of vestigial mitochondrial material was often left behind in the residual body, along with other material not incorporated into the daughter parasites (Fig. 5A, +160′). In the related apicomplexan parasite, *Plasmodium falciparum*, the mitochondrion has been reported to physically associate with the apicoplast throughout the asexual cycle (Hopkins et al., 1999; van Dooren et al., 2005). Apicoplast-mitochondrial association was also observed in *T. gondii* at the time of apicoplast elongation (Fig. 5B,C), providing the potential for metabolic interaction, but this association was not maintained continuously throughout the cell cycle. Dividing apicoplasts enter daughter parasites early during IMC formation (see Fig. 2N, corresponding to +60′ in Fig. 5A), well before mitochondrial entry (~120′ in Fig. 5A). The same sequence of events was observed in living cells by time-lapse microscopy

using parasites stably expressing FNR_L-*Ds*Red and $HSP60_L$-YFP, or ACP_L-EGFP and $HSP60_L$-*Ds*Red, to label the apicoplast and mitochondrion, respectively (not shown).

The migration and segregation of subcellular organelles is likely to require interaction with cytoskeletal elements. Actin appears not to be involved, because parasites grown for 24 hours in 1 μM cytochalasin D [in the cytochalasin-resistant human epithelial cell line Cyt-1 (Toyama and Toyama, 1984)] exhibited normal organellar partitioning (not shown). The dinitroaniline herbicide oryzalin specifically inhibits the formation of certain microtubule subsets in *T. gondii,* without affecting host cell microtubules (Stokkermans et al., 1996; Morrissette and Sibley, 2002). Although oryzalin completely blocks polymerization of subpellicular microtubules and the formation of daughter parasite scaffolds, DNA replication and centriole duplication proceeded normally, as did division of the Golgi complex (Fig. 6, row 1, right). The loss of subpellicular microtubules prevents daughter scaffold formation and karyokinesis,resulting in giant cells containing multiple centrioles and a multilobed polyploid nucleus (Striepen et al., 2000; Morrissette and Sibley, 2002), but paired Golgi were nevertheless evident, remaining in close association with the nucleus in the absence of developing daughters (arrowheads). By contrast, later events were at least indirectly dependent on microtubules. The apicoplast was able to elongate, but typically failed to divide (Fig. 6, row 2) (see also Striepen et al., 2000). The ER formed normal ruffles and extensions, but could not divide in the absence of nuclear division, although some material did associate with IMC aggregates (Fig. 6, row 3). Mitochondrial reticulation was also evident (Fig. 6, row 4), but these organelles failed to divide in oryzalin-treated parasites.

Discussion

We have exploited a variety of native and heterologous targeting signals fused to various fluorescent protein reporters, to engineer transgenic *T. gondii* parasites that may yield insights into the mechanism of organellar replication and the remarkable process of intracellular daughter parasite assembly in protists of the phylum Apicomplexa. IMC1-based markers provide a particularly useful set of landmarks, because this filament protein (Mann and Beckers, 2001) – which is conserved in *Plasmodium* species and other apicomplexan parasites (Khater et al., 2004) – forms an integral part of the scaffold upon which daughter parasites are assembled (Fig. 1) (Hu et al., 2002). Colocalization of multiple markers in living parasites has been used to construct a model of organellar events throughout the ~6.5 hour *T. gondii* tachyzoite life cycle, as shown in Fig. 7 (key events are also summarized in Table 1). Note that the packaging of subcellular organelles is strictly coordinated, invariably proceeding in the following order: centriole and Golgi → apicoplast → nucleus and ER → mitochondrion; rhoptries and micronemes are synthesized de novo in each daughter cell.

The centriole is located near the Golgi and apicoplast in interphase cells (Fig. 2C), but migrates around the nucleus at the onset of mitosis (Fig. 2F), and replicates (Fig. 2I) before returning to the apical juxtanuclear region at approximately the same time as Golgi division and apicoplast elongation (Fig. 2J,K,L). Although centrioles are associated with the apicoplast through most of the cell cycle (Striepen et al., 2000), their migration results in a period of ~1 hour where they are not associated with the ends of replicating Golgi or elongating apicoplasts (cf. Fig. 2F,G,H,I and Fig. 7) (Hartmann et al., 2006). The

significance of centriole migration is not clear. Microtubule-mediated centriole or spindle pole motility and repositioning have been suggested to be important for many biological processes, including directional cell motility (Ueda et al., 1997), completion of cytokinesis (Piel et al., 2001) and delivery of secretory granules to the immunological synapses (Stinchocombe et al., 2006) (for reviews, see Hoyt, 2000; Manneville and Etienne-Manneville, 2006). Because two daughter cells form in various orientations irrespective of the mother's apical-basal axis (cf. Fig. 2M), and the migration occurs around the nucleus before the daughter scaffold formation, the centriole migration may be involved in defining the apical-basal polarity of daughter cells and subcellular structures. Further molecular and cellular characteristics of centriole separation and migration with respect to the polarity of daughter parasites are currently being investigated.

Elongation of both the Golgi (Fig. 2D) and apicoplast (Fig. 2E) begins prior to the initiation of daughter scaffold formation (Fig. 2J,K). At this stage, the apicoplast is often associated with the mitochondrion (Fig. 5B). Golgi fission (Fig. 2G) also precedes the initiation of daughter scaffold formation, and the developing scaffold immediately envelops the Golgi. All events up to this stage take place even in the presence of oryzalin (Fig. 6), which blocks the formation of subpellicular microtubules and organization of IMC that defines developing daughter parasites (Stokkermans et al., 1996;Morrissette and Sibley, 2002). The IMC is comprised of flattened vesicles, presumably derived from the Golgi complex (Porchet and Torpier, 1977; Dubremetz and Torpier, 1978; Nichols and Chiappino, 1987; Morrissette et al., 1997). Division of the apicoplast, ER and nucleus occur later, and the morphology of these processes suggests a link between elongation of the daughter scaffold and the segregation of these organelles. Consistent with this hypothesis, only the Golgi complex (Fig. 6, row 1) and centriole (Striepen et al., 2000) divide in oryzalin-treated cells.

The cytoskeletal scaffolding for progeny *T. gondii* parasites is initiated with the formation of two daughter conoids (Swedlow et al., 2002; Hu et al., 2006). This occurs before completion of DNA synthesis (Radke et al., 2001; Hu et al., 2002; Hu et al., 2004), and is presumed to nucleate IMC assembly (Fig. 2J,K). *Plasmodium* parasites lack an intact conoid, but retain the apical polar rings, which probably nucleate subpellicular microtubule polymerization (Russell and Sinden, 1982; Kaidoh et al., 1993). As daughter scaffolds elongate, DNA replication is completed, and the nucleus lobulates (Fig. 2N,O), coincident with formation of the intranuclear spindle (Swedlow et al., 2002) and the ramification of both the ER and mitochondrion (Fig. 3, Fig. 5A). Growth of the IMC scaffold first encapsulates the daughter centrioles and Golgi, followed by the apicoplast, and then the nucleus and ER (Fig. 2). Immature rhoptries and micronemes – specialized secretory organelles associated with host cell attachment, invasion, and virulence (Carruthers and Sibley, 1997; Taylor et al., 2006; Saeij et al., 2006; Saeij et al., 2007) – then begin to form de novo, within the developing parasites (Fig. 4). Interestingly, the mitochondrion is excluded from the daughter parasites until very late in the division process (Fig. 5A). Daughter parasites ultimately acquire their plasma membrane by budding out from the mother, leaving behind any unencapsulated material as a residual body (cf. Fig. 6, left, bottom two panels).

It is interesting that the parasite mitochondrion and plastid both replicate in concert with cell division, unlike the autonomous replication of these organelles in most eukaryotes (Kuroiwa

et al., 1998; Pyke, 1999; Osteryoung, 2001; Yoon and McNiven, 2001). A precedent may be found in the red alga *Cyanidioschyzon merolae* (Suzuki et al., 1994; Kuroiwa, 2000; Miyagishima et al., 2001), which also replicates its mitochondrion and plastid in synchrony with nuclear mitosis. Although these organisms are phylogenetically unrelated, and differ in the precise mechanism of both organellar and nuclear division, each species possesses only a single mitochondrion and a single plastid, placing a premium on high-fidelity segregation.

Mitochondria in algae and chloroplasts (like their α-proteobacterial and cyanobacterial ancestors) replicate by binary fission, a process associated with electron-dense rings containing ftsZ-related proteins (Osteryoung, 2001). The presence of such electron-dense rings in apicomplexans remains debatable (Bannister et al., 2000a; Matsuzaki et al., 2001; Ferguson et al., 2005), and no ftsZ orthologs are evident in the *P. falciparum* or *T. gondii* genome databases (Aurrecoechea et al., 2007). By contrast, the dynamin GTPase Dnm1p/Drp1 is involved in mitochondrial fission in yeast and mammalian systems (Cerveny et al., 2007). Although the *T. gondii* genome encodes two dynamin GTPases (Gene IDs 57.m01879 and 645.m00325), phylogenic analysis suggests that they are only distantly related to Dnm1p/Drp1 or Vps1p. In addition, 57.m01879 fused to a fluorescent protein appears to be distributed throughout the parasite. Our attempts at transient overexpression of putative dominant-negative mutants have not been successful (not shown).

In *P. falciparum*, the apicoplast and mitochondrion remain associated with each other throughout the asexual cycle (Hopkins et al., 1999; van Dooren et al., 2005). The mitochondrion and chloroplast are also found in close proximity and divide concurrently in the red algae *C. merolae* (Suzuki et al., 1994). In this study, we found that the *T. gondii* apicoplast and mitochondrion associate transiently, during the G1 and apicoplast elongation stages before daughter cell formation. Since these two organelles interact functionally (e.g. for heme biosynthesis), direct interaction between the apicoplast and mitochondrion may facilitate transfer of metabolic intermediates between these compartments.

The late entry of the mitochondrion into the developing daughter cell (Fig. 5A, +110–120′) is quite distinct from the timing of apicoplast replication (Fig. 2, middle column). Movement of the mitochondrion into developing daughters may depend on cytoskeletal filaments and motors associated with the IMC, including intermediate filaments and microtubules (Mann and Beckers, 2001; Hu et al., 2002; Morrissette and Sibley, 2002). Mitochondrial movement depends on microtubules and their motors (e.g. kinesin 1) in many multicellular organisms, and on actin filaments and Arp2/3-complex-dependent actin polymerization in yeasts (reviewed by Boldogh and Pon, 2007). Intermediate filaments have also been implicated in mitochondrial movement in neuronal cells [neurofilaments (Wagner et al., 2003)], muscle cells [desmin (Milner et al., 2000)], and in *Saccharomyces cerevisiae*, where mutation of the intermediate-filament-like protein Mdm1p causes mitochondrial fragmentation, resulting in defective organellar transfer into daughter buds (McConnell et al., 1990; McConnell and Yaffe, 1993). Although no orthologs of these intermediate filament proteins are evident in *T. gondii* and *Plasmodium* spp., other intermediate-filament-like proteins – such as IMC1 – may be involved in mitochondrial distribution. In this study, we demonstrate that even under oryzalin treatment, the mitochondrion in *T. gondii* can extend and associate with local concentrations of IMC (Fig. 6, row 4, right). The majority of actin in apicomplexan parasites

is found in monomeric form (Dobrowolski et al., 1997), and cytochalasin D has no effect on mitochondrial distribution in *T. gondii* (not shown).

The role (if any) of the residual body in organelle partitioning is unclear. On the basis of studies using the actin-filament-destabilizing agent cytochalasin D, Shaw et al. (Shaw et al., 2000) suggested that actin has no effect on parasite replication, but rather alters organelle turnover resulting in large residual bodies containing various organelles. Overexpression of MyoB has also been reported to increase the size of the residual body (Delbac et al., 2001). These may be nonspecific effects, however, as we have observed similar enhancement of residual body formation in response to various treatments (chloramphenicol, low temperature, etc.); it appears that any treatment reducing the efficiency of daughter cell assembly increases residual body size. We have also screened available cell cycle mutants, and parasites transiently transfected with a dominant-negative Rab GTPase, which may be involved in IMC formation, but none of these appears to affect organelle segregation specifically (data not shown).

How to build a parasite? Unlike most other eukaryotes, apicomplexan species contain only a single copy of many intracellular organelles, providing an appealing model system for studies on eukaryotic organellar replication (Hager et al., 1999; Striepen et al., 2000; Joiner and Roos, 2002; Pelletier et al., 2002; Hartmann et al., 2006). However, unlike most prokaryotic and eukaryotic cells, apicomplexans replicate not by binary fission, but rather by assembling daughter cells within the mother – a process conceptually more closely analogous to viral self-assembly. This organization offers many attractive features, including high-fidelity delivery of single-copy organelles to dividing daughter cells, a highly polarized organization (required for host cell invasion, and therefore survival) and the ability to dispose of waste products by default – simply leaving behind unwanted material (such as the polymerized heme produced by hemoglobin digestion in malaria parasites) with the mother cell carcass, obviating the need for lysosomes (Shaw et al., 1998). Ensuring the fidelity of such a regimented cell assembly process undoubtedly requires careful regulation. Given the unusual nature of the parasite cell cycle, in which events associated with M phase and division in a typical eukaryotic cell (organellar replication, karyokinesis, mitosis, cytokinesis) span >75% of the parasite cell cycle, completely encompassing S phase, it will be interesting to exploit the accessibility of *T. gondii* to molecular genetic and cell biological manipulation (Roos et al., 1994; Striepen and Soldati, 2007), and the recent completion of the parasite genome (Aurrecoechea et al., 2007), to explore mechanisms of cell cycle control (Radke and White, 1998; Hu et al., 2004).

Materials and Methods

Parasites and cell culture

Tachyzoites derived from the RH strain of *T. gondii* were maintained by serial passage in human foreskin fibroblast (HFF) cell monolayers cultured in Modified Eagle's Medium (MEM, Gibco) supplemented with 1% heat-inactivated fetal bovine serum (Ed1) at 37°C and 5% CO_2 in a humidified incubator, as previously described (Roos et al., 1994). For experiments with oryzalin (stock solution 10 mM in DMSO, DowElanco), 3–5310^5 parasites were inoculated into HFF monolayers grown on 22 glass coverslips and incubated without

drugs for 12–16 hours. Oryzalin was then added to a final concentration of 1 μM, and parasites were cultivated 24 hours after drug addition. For experiments with cytochalasin D (stock solution 1 mM in DMSO, Sigma), sub-confluent human epithelial cell lines KB and Cyt-1 (Toyama and Toyama, 1984) grown on 22 mm glass coverslips were infected with parasites for 1 hour. Coverslips were washed extensively with Ed1 medium to remove extracellular parasites and cytochalasin D in Ed1 medium was added to coverslips with Cyt-1 cells only to a final concentration of 1 μM and parasites were cultivated for an additional 24 hours.

Molecular methods

The following conventions are used for describing primer sequences: underlining indicates restriction sites, capitalization indicates stop or start codons, bold indicates introduced coding sequence. All expression vectors used in this study are based on the pBluescript II KS^+ backbone (Stratagene) with recombinant sequences inserted between the 59 *Hin*dIII and 39 *Not*I sites. Except where otherwise noted, all plasmids include the following domains: (1) a *Hin*dIII-*Bgl*II fragment containing a promoter derived from *T. gondii* α-tubulin or DHFR-TS; the *Bgl*II site lies upstream of the initiation codon (typically …agatctaaaATG…). (2) A *Bgl*II-*Avr*II fragment containing protein coding sequence (ACP_L, FNR_L, GRASP, $HSP60_L$, IMC1 or $P30_L$); the L subscript indicates use of a truncated protein that is sufficient to mediate targeting: apicoplast targeting signals are from ACP and FNR, the mitochondrial targeting signal is from HSP60. (3) An *Avr*II-*Pst*I (or *Avr*II-*Afl*II) fragment containing a fluorescent protein reporter (GFP, YFP, *Ds*Red, mRFP), sometimes fused to a C-terminal epitope for targeting (e.g. HDEL) (Hager et al., 1999). (4) A *Pst*I (or *Afl*II)-*Not*I fragment containing 39 sequences derived from *T. gondii* DHFR-TS. (5) An optional *sag*CAT*sag* cassette, for chloramphenicol selection of stable transgenics.

Construction methods have previously been described for the basic GFP-expressing vector p*dhfr*CAT-GFP, and the secretion vectors p*tub*$P30_L$-GFP and p*tub*$P30_L$-YFP (Striepen et al., 1998; Matrajt et al., 2002), as well as constructs that label the ER (p*tub*$P30_L$-GFP-HDEL) (Hager et al., 1999), Golgi (p*tub*GRASP-YFP) (Pelletier et al., 2002), IMC (p*tub*IMC1-YFP) (Hu et al., 2002), micronemes (p*tub*MIC3-GFP) (Striepen et al., 1998), rhoptries (p*tub*ROP1-CAT-YFP) (Dzierszinski et al., 2004) and apicoplast [p*tub*ACP_L-EGFP (Waller et al., 1998); p*tub*FNR_L-YFP (Striepen et al., 2000; Harb et al., 2004); p*tub*FNR_L-*Ds*Red (He et al., 2001)]. For labeling the mitochondrion, sequences encoding the 55 N-terminal residues of *T. gondii* heatshock protein 60 (Toursel et al., 2000) were amplified from tachyzoite cDNA using primers 59-atgcagatctaaaATGcttgcccgcgcttca-39 and 59-cagtcctagggccgagagtgactccgac-39, and introduced as a *Bgl*II-*Avr*II fragment into p*tub*IMC1-YFP and p*tub*FNR_L-*Ds*Red, yielding p*tub*$HSP60_L$-YFP and p*tub*$HSP60_L$-*Ds*Red, respectively.

Because the *Pst*I site used to separate coding from 39 noncoding sequences is also present in the upstream polylinker, a new plasmid was engineered to replace the downstream *Pst*I with a unique *Afl*II restriction site. The *Bgl*II-*Pst*I domain from p*tub*ACP_L-EGFP was replaced by a fragment obtained by amplification using primers 59-ggaagatctaaaATGgagatgcatccccgcaacgc-39 and 59-ctagctgcag*cttaag*cttgtacagc-

tcgtccatgccgagagtgatc-39. The resulting plasmid was digested with *Afl*II and *Not*I, and 39 flanking sequences were replaced by a fragment amplified using primers 59-tagcttaagTAAacagaagctgcccgtctctcg-39 and 59-taatacgactcactataggg-39 (from the T7 promoter region downstream of the *Not*I site), to yield p*tub*ACP$_L$-EGFP(*Afl*).p*tub*FNR$_L$-YFP-6xHis was constructed using primers 59-tgcagatctacaATGgttcgg-ggcatccgtcctc-39 and 59-tgacttaagTTA**gtgatggtggtgatggt***gg*ctagccttgtacagctcgtcca-tgccgagag-39 to amplify FNR$_L$-YFP from p*tub*FNR$_L$-YFP, introducing a *Nhe*I site followed by six histidine codons immediately upstream of the termination codon. Plasmid p*tub*FNR$_L$-mRFP was constructed by replacing the YFP-63His domain with a fragment amplified from plasmid pRSET-mRFP1 (kindly provided by R. Tsien, University of California, San Diego, CA) (Campbell et al., 2002) using primers 59-atgcgtccctagggcctcctccgaggacgtcatc-39 and 59-ctgcatcttaagTTAggcgccggtggagtgg-cggcc-39 to amplify mRFP. Plasmids p*tub*GRASP-mRFP, p*tub*IMC1-mRFP and p*tub*ACP$_L$-mRFP were constructed by replacing FNR$_L$ with GRASP, IMC1 and ACP$_L$ from a *Bgl*II/*Avr*II digestion of p*tub*GRASP-YFP, p*tub*IMC1-YFP and p*tub*ACP$_L$-EGFP, respectively. Plasmids p*tub*ACP$_L$-YFP and p*tub*ACP$_L$-*Ds*Red were constructed by replacing FNR$_L$ in p*tub*FNR$_L$-YFP and p*tub*FNR$_L$-*Ds*Red with ACP$_L$ in p*tub*ACP$_L$-EGFP via *Bgl*II-*Avr*II digestion. Plasmid p*tub*P30$_L$-YFP-HDEL was constructed using *Bgl*II-*Afl*II fragment amplified from a P30$_L$-YFP plasmid using primers 59-ggaagatctATGtcggtttcgctgcac-39 and 59-gcatcttaagCTA**caactcgtcgtg**cttgtacagctcgtcc-39; p*tub*P30$_L$-mRFP-HDEL was constructed by replacing YFP-HDEL with mRFP-HDEL, obtained by amplification using primers 59-atgccctagggcctcctccgaggacgtcat-caag-39 and 59-ctgcatcttaagCTA**caactcgtcgtg**ggcgccggtggagtggcggcc-3'.

High-level expression of centrin under control of the tubulin promoter produced large amounts of cytosolic protein (data not shown). The *Bgl*II-*Not*I fragment from plasmid p*dhfr* CAT-GFP (Matrajt et al., 2002) was therefore replaced with the sequences from p*tub*ACP$_L$-EGFP(*Afl*), to yield p*dhfr*ACP$_L$-EGFP(*Afl*). EGFP-*Homo sapiens* (*Hs*) Centrin was amplified from pEGFP-CENT2 (White et al., 2000) using primers 59-gctagggatccgctagcaaaATGgtgagcaagggcgaggagctg-39 and 59-gtca-cttaagTTAatagaggctggtctttttcatg-39, and introduced as a *Bam*HI-*Afl*II fragment into *Bgl*II-*Afl*II-digested p*dhfr*ACP$_L$-EGFP(*Afl*), yielding p*dhfr*EGFP-*Hs*Centrin, with a 59 *Nhe*I site in place of the original *Bgl*II site, and a unique *Bgl*II site between EGFP and *Hs*Centrin. Finally, *Hs*Centrin was replaced with *T. gondii* centrin amplified from a *T. gondii* cDNA using primers 59-cgatagatctcatagtcggaaaggagcgagctctc-39 and 59-acgtcttaagCTAgaacagattcgtctttctcatgat-39 (based on sequences obtained from ToxoDB.org), to yield plasmid p*dhfr*EGFP-*Tg*Centrin, which places centrin expression under control of the weaker DHFR promoter.

Transfections were performed as previously described (Roos et al., 1994). Briefly,10^7 parasites were electroporated (2-mm-gap cuvette, BTX; 1.5 keV pulse, 24 Ω) with 50 μg plasmid DNA containing a *sag*CAT*sag* cassette for selection in 20 μM chloramphenicol, or cotransfected with 5 μg pDHFR-TSc3 for selection in 1 μM pyrimethamine, and individual clones were isolated by limiting dilution. The following stable, clonal parasite cell lines were obtained by selection in chloramphenicol: P30$_L$-mRFP-HDEL, GRASP-mRFP, IMC1-YFP (Hu et al., 2002), ACP$_L$-EGFP (Striepen et al., 2000), FNR$_L$-*Ds*Red (He et al., 2001),

FNR_L-mRFP, ACP_L-mRFP, $HSP60_L$-YFP, and $HSP60_L$-*Ds*Red; the following lines were obtained by selection in pyrimethamine: $P30_L$-YFP-HDEL and EGFP-*Tg*Centrin (Hartmann et al., 2006). The following doubly resistant transgenic lines were isolated by selection in chloramphenicol followed by pyrimethamine: IMC1-YFP/$P30_L$-mRFP-HDEL, IMC1-YFP/GRASP-mRFP, IMC1-YFP/$HSP60_L$-*Ds*Red, FNR_L-*Ds*Red/$HSP60_L$-YFP, and ACP_L-EGFP/$HSP60_L$-*Ds*Red. In some experiments, colocalization and analysis of organellar association was also carried out by transient transfection of stably-transformed parasites.

Microscopy

For fixed fluorescence analyses, 3–5310^5 parasites were inoculated onto confluent HFF cell monolayers grown on 22 mm glass coverslips, and examined after incubation for 24–32 hours at 37°C. Coverslips were then fixed in 3.7% paraformaldehyde and permeabilized with 0.25% Triton X-100 in PBS (phosphate-buffered saline). For immunofluorescence assay, rabbit polyclonal anti-ACP antibody (Waller et al., 1998) (1:1000) was used followed by Alexa Fluor 594-conjugated goat anti-rabbit antibody (1:5000) (Invitrogen). For DNA labeling, coverslips were incubated after permeabilization in 2.8 μM 49,6-diamidino-2-phenylindole dihydrochloride (DAPI, Invitrogen) in PBS for 5 minutes and washed twice with PBS. Coverslips were mounted with Fluoromount G (Southern Biotechnology Associates). For time-lapse microscopy, 3–5310^5 parasites were inoculated into confluent HFF cell monolayers grown in glass-bottomed dishes (MatTek) and incubated at 37°C for 16–24 hours. Media was buffered with 25 mM HEPES pH 7.0 (Gibco) immediately prior to examination at 37°C using a humidified observation chamber (Murray, 2003).

Image stacks were collected using an Olympus IX70 inverted microscope equipped with a 100W Hg-vapor lamp with appropriate barrier or emission filters (DeltaVision). Images were captured using a CoolSNAP HQ cooled-CCD camera (Photometrics) and DeltaVision softWorx software (Applied Precision). All image stacks were deconvolved to remove the effects of fluorescence arising from out-of-focus planes using DeltaVision softWorx software (Applied Precision).

Supplementary Material

Refer to Web version on PubMed Central for supplementary material.

Acknowledgments

We wish to thank Roger Tsien (UCSD) for pRSET-mRFP, Graham Warren (University of Vienna) for providing p*tub*GRASP-YFP plasmid and serial sections of transmission electron microscopic images, G. I. McFadden (University of Melbourne) for providing anti-ACP antibody, and Michael Crawford, Florence Dzierinszinski and Omar Harb for helpful suggestions. This work was supported by research grants from the NIH.

References

Aikawa M (1971). Parasitological review. *Plasmodium:* the fine structure of malarial parasites. Exp. Parasitol 30, 284–320. [PubMed: 4399774]

Aurrecoechea C, Heiges M, Wang H, Wang Z, Fischer S, Rhodes P, Miller J,Kraemer E, Stoeckert CJ Jr, Roos DS et al. (2007). ApiDB: integrated resources for the apicomplexan bioinformatics resource center. Nucleic Acids Res 35, D427–D430. [PubMed: 17098930]

Bannister LH, Hopkins JM, Fowler RE, Krishna S and Mitchell GH (2000a). A brief illustrated guide to the ultrastructure of *Plasmodium falciparum* asexual blood stages. Parasitol. Today 16, 427–433. [PubMed: 11006474]

Bannister LH, Hopkins JM, Fowler RE, Krishna S and Mitchell GH (2000b).Ultrastructure of rhoptry development in *Plasmodium falciparum* erythrocytic schizonts.Parasitology 121, 273–287. [PubMed: 11085247]

Bereiter-Hahn J and Voth M (1994). Dynamics of mitochondria in living cells: shape changes, dislocations, fusion, and fission of mitochondria. Microsc. Res. Tech 27, 198–219. [PubMed: 8204911]

Boldogh IR and Pon LA (2007). Mitochondria on the move. Trends Cell Biol 17, 502–510. [PubMed: 17804238]

Campbell RE, Tour O, Palmer AE, Steinbach PA, Baird GS, Zacharias DA and Tsien RY (2002). A monomeric red fluorescent protein. Proc. Natl. Acad.Sci. USA 99, 7877–7882. [PubMed: 12060735]

Carruthers VB and Sibley LD (1997). Sequential protein secretion from three distinct organelles of *Toxoplasma gondii* accompanies invasion of human fibroblasts. Eur. J. Cell Biol 73, 114–123. [PubMed: 9208224]

Cerveny KL, Tamura Y, Zhang Z, Jensen RE and Sesaki H (2007). Regulation of mitochondrial fusion and division. Trends Cell Biol 17, 563–569. [PubMed: 17959383]

Delbac F, Sänger A, Neuhaus EM, Stratmann R, Ajioka JW, Toursel C, Herm-Götz A, Tomavo S, Soldati T and Soldati D (2001). *Toxoplasma gondii* myosins B/C: one gene, two tails, two localizations, and a role in parasite division. J. Cell Biol 155, 613–624. [PubMed: 11706051]

Dobrowolski JM, Niesman IR and Sibley LD (1997). Actin in the parasite *Toxoplasma gondii* is encoded by a single copy gene, ACT1 and exists primarily in a globular form. Cell Motil. Cytoskeleton 37, 253–262. [PubMed: 9227855]

Dubremetz JF and Torpier G (1978). Freeze fracture study of the pellicle of an Eimerian sporozoite (Protozoa, Coccidia). J. Ultrastruct. Res 62, 94–109. [PubMed: 418187]

Dubremetz JF, Garcia-Reguet N, Conseil V and Fourmaux MN (1998). Apical organelles and host-cell invasion by Apicomplexa. Int. J. Parasitol 28, 1007–1013. [PubMed: 9724870]

Dzierszinski F, Nishi M, Ouko L and Roos DS (2004). Dynamics of *Toxoplasma gondii* differentiation. Eukaryotic Cell 3, 992–1003. [PubMed: 15302832]

Ferguson DJ, Henriquez FL, Kirisits MJ, Muench SP, Prigge ST, Rice DW, Roberts CW and McLeod RL (2005). Maternal inheritance and stage-specific variation of the apicoplast in *Toxoplasma gondii* during development in the intermediate and definitive host. Eukaryotic Cell 4, 814–826. [PubMed: 15821140]

Fichera ME, Bhopale MK and Roos DS (1995). In vitro assays elucidate the peculiar kinetics of clindamycin action against *Toxoplasma gondii*. Antimicrob. Agents Chemother 39, 1530–1537. [PubMed: 7492099]

Foth NJ and McFadden GI (2003). The apicoplast: a plastid in *Plasmodium falciparum* and other apicomplexan parasites. Int. Rev. Cytol 224, 54–57.

Hager KM, Striepen B, Tilney LG and Roos DS (1999). The nuclear envelope serves as an intermediary between the endoplasmic reticulum and Golgi complex in the intracellular parasite *Toxoplasma gondii*. J. Cell Sci 112, 2631–2638. [PubMed: 10413671]

Harb OS, Chatterjee B, Fraunholz MJ, Crawford MJ, Nishi M and Roos DS (2004). Multiple functionally redundant signals mediate targeting to the apicoplast in the apicomplexan parasite *Toxoplasma gondii*. Eukaryotic Cell 3, 663–674. [PubMed: 15189987]

Hartmann J, Hu K, He CY, Pelletier L, Roos DS and Warren G (2006). Golgi and centrosome cycles in *Toxoplasma gondii*. Mol. Biochem. Parasitol 145, 125–127. [PubMed: 16266757]

He CY, Striepen B, Pletcher CH, Murray JM and Roos DS (2001). Targeting and processing of nuclear-encoded apicoplast proteins in plastid segregation mutants of *Toxoplasma gondii*. J. Biol. Chem 276, 28436–28442. [PubMed: 11319231]

Hopkins J, Fowler R, Krishna S, Wilson I, Mitchell G and Bannister L (1999).The plastid in Plasmodium falciparum asexual blood stages: a three-dimensional ultrastructural analysis. Protist 150, 283–295. [PubMed: 10575701]

Hoyt MA (2000). Exit from mitosis: spindle pole power. Cell 102, 267–270. [PubMed: 10975516]

Hu K, Mann T, Striepen B, Beckers CJ, Roos DS and Murray JM (2002). Daughter cell assembly in the protozoan parasite *Toxoplasma gondii*. Mol. Biol. Cell 13, 593–606. [PubMed: 11854415]

Hu K, Roos DS, Angel SO and Murray JM (2004). Variability and heritability of cell division pathways in *Toxoplasma gondii*. J. Cell Sci 117, 5697–5705. [PubMed: 15494366]

Hu K, Johnson J, Florens L, Fraunholz M, Suravajjala S, Dilullo C, Yates J,Roos DS and Murray JM (2006). Cytoskeletal components of an invasion machine:the apical complex of *Toxoplasma gondii*. PLoS Pathogens 2, e13. [PubMed: 16518471]

Joiner KA and Roos DS (2002). Secretory traffic in *Toxoplasma gondii*: less is more.J. Cell Biol 156, 1039–1050. [PubMed: 11901169]

Kaidoh T, Nath J, Okoye V and Aikawa M (1993). Novel structure in the pellicular complex of *Plasmodium falciparum* gametocytes. J. Eukaryot. Microbiol 40, 269–271. [PubMed: 8508166]

Khater EI, Sinden RE and Dessens JT (2004). A malaria membrane skeleton protein is essential for normal morphogenesis, motility, and infectivity of sporozoites. J. Cell Biol 167, 425–432. [PubMed: 15533999]

Köhler S, Delwiche CF, Denny PW, Tilney LG, Webster P, Wilson RJM, Palmer JD and Roos DS (1997). A plastid of probable green algal origin in apicomplexan parasites. Science 275, 1485–1488. [PubMed: 9045615]

Kuroiwa T (2000). The discovery of the division apparatus of plastids and mitochondria.J. Electron Microsc. Tokyo 49, 123–134. [PubMed: 10791428]

Kuroiwa T, Kuroiwa H, Sakai A, Takahashi H, Toda K and Itoh R (1998). The division apparatus of plastids and mitochondria. Int. Rev. Cytol 181, 1–41. [PubMed: 9522454]

Logan DC (2006). Plant mitochondrial dynamics. Biochem. Biophys. Acta 1763, 430–441. [PubMed: 16545471]

Mann T and Beckers C (2001). Characterization of the subpellicular network, a filamentous membrane skeletal component in the parasite *Toxoplasma gondii*. Mol. Biochem. Parasitol 115, 257–268. [PubMed: 11420112]

Manneville J and Etienne-Manneville S (2006). Positioning centrosomes and spindle poles: looking at the periphery to find the centre. Biol. Cell 98, 557–565. [PubMed: 16907664]

Matrajt M, Nishi M, Fraunholz MJ, Peter O and Roos DS (2002). Amino-terminal control of transgenic protein expression levels in *Toxoplasma gondii*. Mol. Biochem. Parasitol 120, 285–289. [PubMed: 11897133]

Matsuzaki M, Kikuchi T, Kita K, Kojima S and Kuroiwa T (2001). Large amounts of apicoplast nucleoid DNA and its segregation in *Toxoplasma gondii*. Protoplasma 218, 180–191. [PubMed: 11770434]

McConnell SJ and Yaffe MP (1993). Intermediate filament formation by a yeast protein essential for organelle inheritance. Science 260, 687–689. [PubMed: 8480179]

McConnell SJ, Stewart LC, Talin A and Yaffe MP (1990). Temperature-sensitive yeast mutants defective in mitochondrial inheritance. J. Cell Biol 111, 967–976. [PubMed: 2202739]

Melo EJ, Attias M and De Souza W (2000). The single mitochondrion of tachyzoites of *Toxoplasma gondii*. J. Struct. Biol 130, 27–33. [PubMed: 10806088]

Milner DJ, Mavroidis M, Weisleder N and Capetanaki Y (2000). Desmin cytoskeleton linked to muscle mitochondrial distribution and respiratory function. J. Cell Biol 150, 1283–1298. [PubMed: 10995435]

Miyagishima S, Kuroiwa H and Kuroiwa T (2001). The timing and manner of disassembly of the apparatuses for chloroplast and mitochondrial division in the red alga *Cyanidioschyzon merolae*. Planta 212, 517–528. [PubMed: 11525508]

Morrissette NS and Sibley LD (2002). Disruption of microtubules uncouples budding and nuclear division in *Toxoplasma gondii*. J. Cell Sci 115, 1017–1025. [PubMed: 11870220]

Morrissette NS, Murray JM and Roos DS (1997). Subpellicular microtubules associate with an intramembranous particle lattice in the protozoan parasite *Toxoplasma gondii*. J. Cell Sci 110, 35–42. [PubMed: 9010782]

Murray JM (2003). Confocal microscopy, deconvolution, and structured illumination methods. In Live Cell Imaging: A Laboratory Manual (ed. Spector DL and Goldman RD), pp. 239–279. New York: Cold Spring Harbor Laboratory Press.

Nichols BA and Chiappino ML (1987). Cytoskeleton of Toxoplasma gondii. J.Protozool 34, 217–226. [PubMed: 3585817]

Ogino N and Yoneda C (1966). The fine structure and mode of division of *Toxoplasma gondii*. Arch. Ophthalmol 75, 218–227. [PubMed: 4159376]

Osteryoung KW (2001). Organelle fission in eukaryotes. Curr. Opin. Microbiol 4, 639–646. [PubMed: 11731314]

Pelletier L, Stern CA, Pypaert M, Sheff D, Ngo HM, Roper N, He CY, Hu K, Toomre D, Coppens I et al. (2002). Golgi biogenesis in *Toxoplasma gondii*. Nature 418, 548–552. [PubMed: 12152082]

Piel M, Nordberg J, Euteneuer U and Bornens M (2001). Centrosome-dependent exit of cytokinesis in animal cells. Science 291, 1550–1553. [PubMed: 11222861]

Porchet E and Torpier G (1977). Etude du germe infectieux de *Sarcocystis tenella* et *Toxoplasma gondii* par la technique du cryodecapage. Z. Parasitenkd 54, 101–124. [PubMed: 415447]

Pyke KA (1999). Plastid division and development. Plant Cell 11, 549–556. [PubMed: 10213777]

Radke JR and White MW (1998). A cell cycle model for the tachyzoite of *Toxoplasma gondii* using the Herpes Simplex Virus thymidine kinase. Mol. Biochem. Parasitol 94, 237–247. [PubMed: 9747974]

Radke JR, Striepen B, Guerini MN, Jerome ME, Roos DS and White MW (2001). Defining the cell cycle for the tachyzoite stage of *Toxoplasma gondii*. Mol.Biochem. Parasitol 115, 165–175. [PubMed: 11420103]

Roos DS, Donald RG, Morrissette NS and Moulton AL (1994). Molecular tools for genetic dissection of the protozoan parasite *Toxoplasma gondii*. Methods Cell Biol 45, 27–78. [PubMed: 7707991]

Roos DS, Crawford MJ, Donald RG, Kissinger JC, Klimczak LJ and Striepen B (1999). Origin, targeting, and function of the apicomplexan plastid. Curr. Opin. Microbiol 2, 426–432. [PubMed: 10458993]

Russell DG and Sinden RE (1982). Three-dimensional study of the intact cytoskeleton of cytoskeleton of coccidian sporozoites. Int. J. Parasitol 12, 221–226. [PubMed: 7076393]

Saeij JP, Boyle JP, Coller S, Taylor S, Sibley LD, Brooke-Powell ET, Ajioka JW and Boothroyd JC (2006). Polymorphic secreted kinases are key virulence factors in toxoplasmosis. Science 314, 1780–1783. [PubMed: 17170306]

Saeij JP, Coller S, Boyle JP, Jerome ME, White MW and Boothroyd JC (2007). *Toxoplasma* co-opts host gene expression by injection of a polymorphic kinase homologue. Nature 445, 324–327. [PubMed: 17183270]

Seeber F, Ferguson DJ and Gross U (1998). *Toxoplasma gondii*: a paraformaldehyde-insensitive diaphorase activity acts as a specific histochemical marker for the single mitochondrion. Exp. Parasitol 89, 137–139. [PubMed: 9603501]

Shaw JM and Nunnari J (2002). Mitochondrial dynamics and division in budding yeast. Trends Cell Biol 12, 178–184. [PubMed: 11978537]

Shaw MK, Roos DS and Tilney LG (1998). Acidic compartments and rhoptry formation in *Toxoplasma gondii*. Parasitology 117, 435–443. [PubMed: 9836308]

Shaw MK, Compton HL, Roos DS and Tilney LG (2000). Microtubules, but not actin filaments, drive daughter cell budding and cell division in *Toxoplasma gondii*. J. Cell Sci 113, 1241–1254. [PubMed: 10704375]

Sheffield HG and Melton ML (1968). The fine structure and reproduction of *Toxoplasma gondii*. J. Parasitol 54, 209–226. [PubMed: 5647101]

Slomianny C and Prensier G (1986). Application of the serial sectioning and tridimensional reconstruction techniques to the morphological study of the *Plasmodium falciparum* mitochondrion. J. Parasitol 72, 595–598. [PubMed: 3537259]

Stinchcombe JC, Majorovits E, Bossi G, Fuller S and Griffiths GM (2006). Centrosome polarization delivers secretory granules to the immunological synapse. Nature 443, 462–465. [PubMed: 17006514]

Stokkermans TJ, Schwartzman JD, Keenan K, Morrissette NS, Tilney LG and Roos DS (1996). Inhibition of *Toxoplasma gondii* replication by dinitroaniline herbicides. Exp. Parasitol 84, 355–370. [PubMed: 8948325]

Striepen B and Soldati D (2007). Genetic manipulation of *Toxoplasma gondii*. In Toxoplasma gondii: The Model Apicomplexan - Perspective and Methods (ed. Weiss LM and Kim K), pp. 391–415. London: Academic Press.

Striepen B, He CY, Matrajt M, Soldati D and Roos DS (1998). Expression, selection, and organellar targeting of the green fluorescent protein in *Toxoplasma gondii*. Mol. Biochem. Parasitol 92, 325–338. [PubMed: 9657336]

Striepen B, Crawford MJ, Shaw MK, Tilney LG, Seeber F and Roos DS(2000). The plastid of *Toxoplasma gondii* is divided by association with the centrosomes.J. Cell Biol 151, 1423–1434. [PubMed: 11134072]

Suzuki K, Ehara T, Osafune T, Kuroiwa H, Kawano S and Kuroiwa T (1994). Behavior of mitochondria, chloroplasts and their nuclei during the mitotic cycle in the ultramicroalga *Cyanidioschyzon merolae*. Eur. J. Cell Biol 63, 280–288. [PubMed: 8082652]

Swedlow JR, Hu K, Andrews PD, Roos DS and Murray JM (2002). Measurement of tubulin content in the conoid and spindle pole of the parasite *Toxoplasma gondii*: a comparison of laser scanning confocal and wide field fluorescence microscopy for quantitative analysis in living cells. Proc. Natl. Acad. Sci. USA 99, 2014–2019. [PubMed: 11830634]

Taylor S, Barragan A, Su C, Fux B, Fentress SJ, Tang K, Beatty WL, Hajj HE, Jerome M, Behnke MS et al. (2006). A secreted serine-threonine kinase determines virulence in the eukaryotic pathogen *Toxoplasma gondii*. Science 314, 1776–1780. [PubMed: 17170305]

Toursel C, Dzierszinski F, Bernigaud A, Mortuaire M and Tomavo S (2000). Molecular cloning, organellar targeting and developmental expression of mitochondrial chaperone HSP60 in *Toxoplasma gondii*. Mol. Biochem. Parasitol 111, 319–332. [PubMed: 11163440]

Toyama S and Toyama S (1984). A variant form of beta-actin in a mutant of KB cells resistant to cytochalasin B. Cell 37, 609–614. [PubMed: 6202424]

Ueda M, Gräf R, MacWilliams HK, Schliwa M and Euteneuer U (1997).Centrosome positioning and directionality of cell movements. Proc. Natl. Acad. Sci.USA 94, 9674–9678. [PubMed: 9275182]

Vaishnava S, Morrison DP, Gaji RY, Murray JM, Entzeroth R, Howe DK and Striepen B (2005). Plastid segregation and cell division in the apicomplexan parasite *Sarcocystis neurona*. J. Cell Sci 118, 3397–3407. [PubMed: 16079283]

van Dooren GG, Marti M, Tonkin CJ, Stimmler LM, Cowman AF and McFadden GI (2005). Development of the endoplasmic reticulum, mitochondrion, and apicoplast during the asexual life cycle of *Plasmodium falciparum*. Mol. Microbiol 157, 405–419.

Wagner OI, Lifshitz J, Janmey PA, Linden M, McIntosh TK and Leterrier JF (2003). Mechanisms of mitochondria-neurofilament interactions. J. Neurosci 23, 9046–9058. [PubMed: 14534238]

Waller RF, Keeling PJ, Donald RG, Striepen B, Handman E, Lang-Unnasch N, Cowman AF, Besra GS, Roos DS and McFadden GI (1998). Nuclear-encoded proteins target to the plastid in *Toxoplasma gondii* and Plasmodium falciparum. Proc. Natl. Acad. Sci. USA 95, 12352–12357. [PubMed: 9770490]

White RA, Pan Z and Salisbury JL (2000). GFP-centrin as a marker for centriole dynamics in living cells. Microsc. Res. Tech 49, 451–457. [PubMed: 10842372]

Yoon Y and McNiven MA (2001). Mitochondrial division: new partners in membrane pinching. Curr. Biol 11, R67–R70. [PubMed: 11231145]

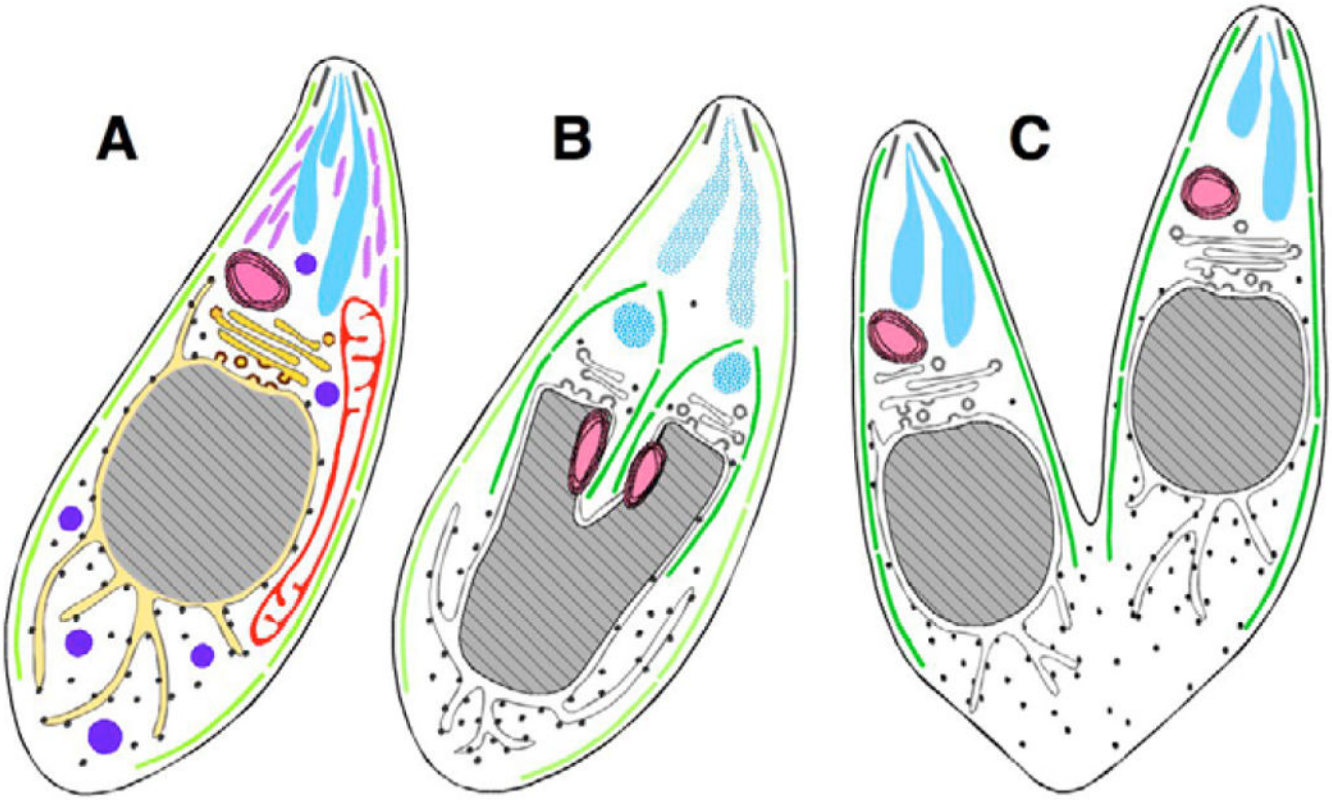

Fig. 1.

Endodyogeny of *Toxoplasma gondii* tachyzoites. Diagrams of longitudinal sections of *T. gondii* parasites at various stages during replication. Subcellular structures (A, interphase) include, proceeding from the apical to the basal end: the conoid (black lines), inner-membrane complex (light green lines), rhoptries (turquoise), micronemes (lavender), dense granules (blue), apicoplast (pink), mitochondrion (red), Golgi (gold) and nucleus (grey), bordered by endoplasmic reticulum (yellow). Mid-way through daughter cell formation (B), the developing daughter IMC scaffolds (dark green) encompass the Golgi and apicoplast (which have already divided), and the nucleus begins to bifurcate. Hatched turquoise indicates breakdown of the maternal rhoptries, and de novo synthesis of daughter rhoptries, which have not yet acquired their mature club-like shape (other organelles not colored and mitochondrion not shown, for clarity). (C) Daughter IMC complexes then grow to establish two complete daughter parasites, which are about to emerge, acquiring their plasma membrane from the mother.

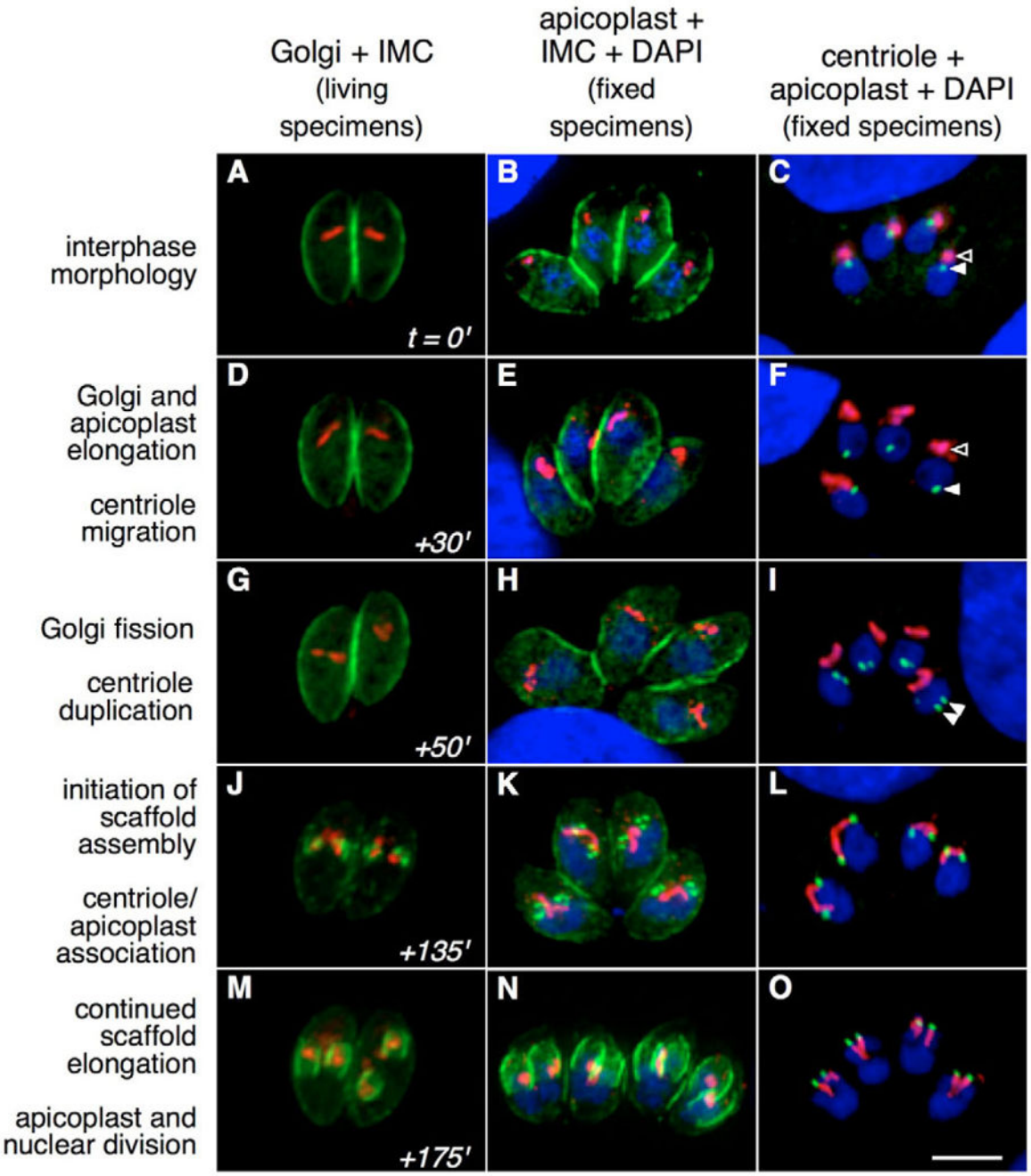

Fig. 2.

Coordination of Golgi, apicoplast, centriolar and nuclear replication. Left column: Time-lapse images of living parasites, labeled for simultaneous visualization of the inner membrane complex of mother and daughter parasites (IMC1-YFP, green) and the Golgi complex (GRASP-mRFP, red). Golgi elongation (D) and fission occurs before the initiation of daughter scaffold formation (J). Daughter Golgi are then encapsulated into the developing daughter parasites (M). Middle column, fixed parasites labeled to image the inner membrane complex (IMC1-YFP, green), apicoplast (anti-ACP, red) and nucleus (DAPI, blue). During interphase, the apicoplast is oval in shape and lies just apical to the nucleus (B). The

apicoplast elongates (E,H) before daughter scaffolds are initiated (K), and finishes dividing near the mid point of scaffold formation, shortly before karyokinesis (N). The same sequence of events was observed in living cells using IMC1-YFP parasites transiently transfected with ACP_L/FNR_L-mRFP/*Ds*Red to label the apicoplast. Right column, fixed parasites labeled to image the centrioles (EGFP-*Tg*Centrin, green), apicoplast (anti-ACP, red) and nucleus (DAPI, blue). The apicoplast (open arrowhead) lies close to the centriole (filled arrowhead) during interphase (C), and begins to elongate (F) before centriole duplication (I). During apicoplast elongation, the centrioles migrate to the basal end of the nucleus (F), where they replicate (I, paired arrowheads) before returning to the apical end (L) and reassociating with the apicoplast, which remains apical throughout. The apicoplast and centrioles remain associated through plastid division (O), nuclear division and cytokinesis. Scale bar: 5 μm.

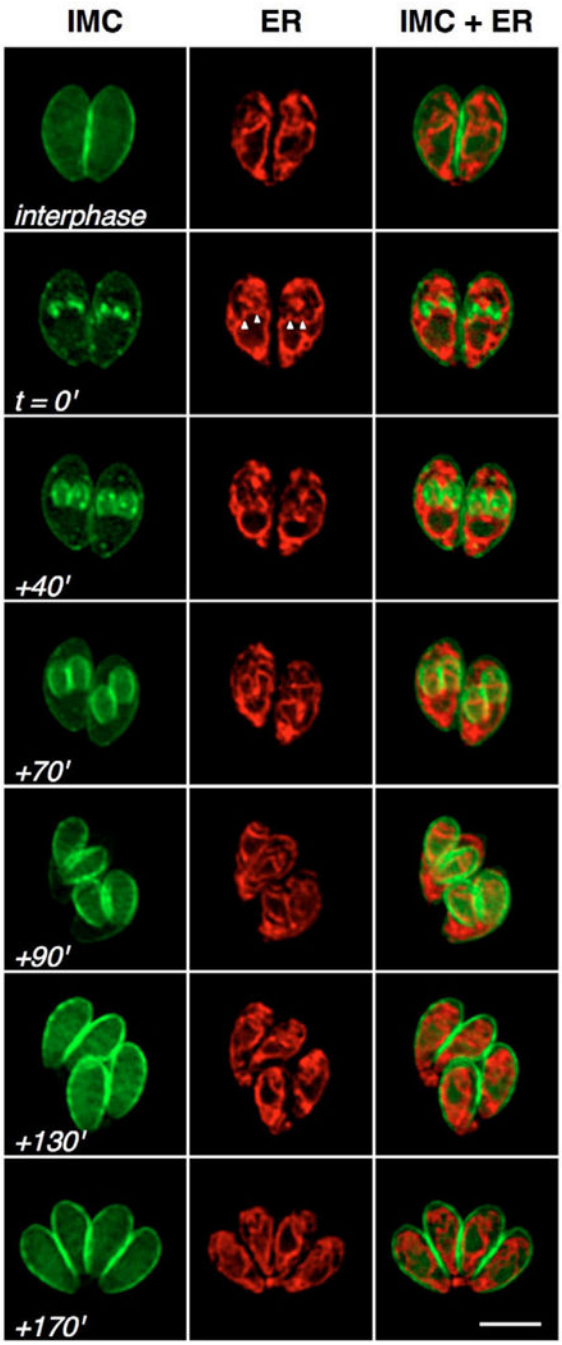

Fig. 3.

Dynamics of ER replication and segregation. Parasites expressing IMC1-YFP (green) and $P30_L$-mRFP-HDEL (red) were examined through the cell cycle using time-lapse microscopy. During interphase (top row), the nucleus is surrounded by the endoplasmic reticulum (ER), from which branches extend both apically and basally. The perinuclear ER expands with the nucleus, and ramifies to form extensive branches coincident with daughter scaffold formation (t=0′). Emanations from the ER associate with the developing IMC (arrowheads; +40′), enter into the developing daughters along with the nucleus (+70′,

+90′), and continue to segregate (+130′) until the emergence of daughter parasites from the mother, leaving a small amount of material behind in the residual body (+170′). Scale bar: 5 μm.

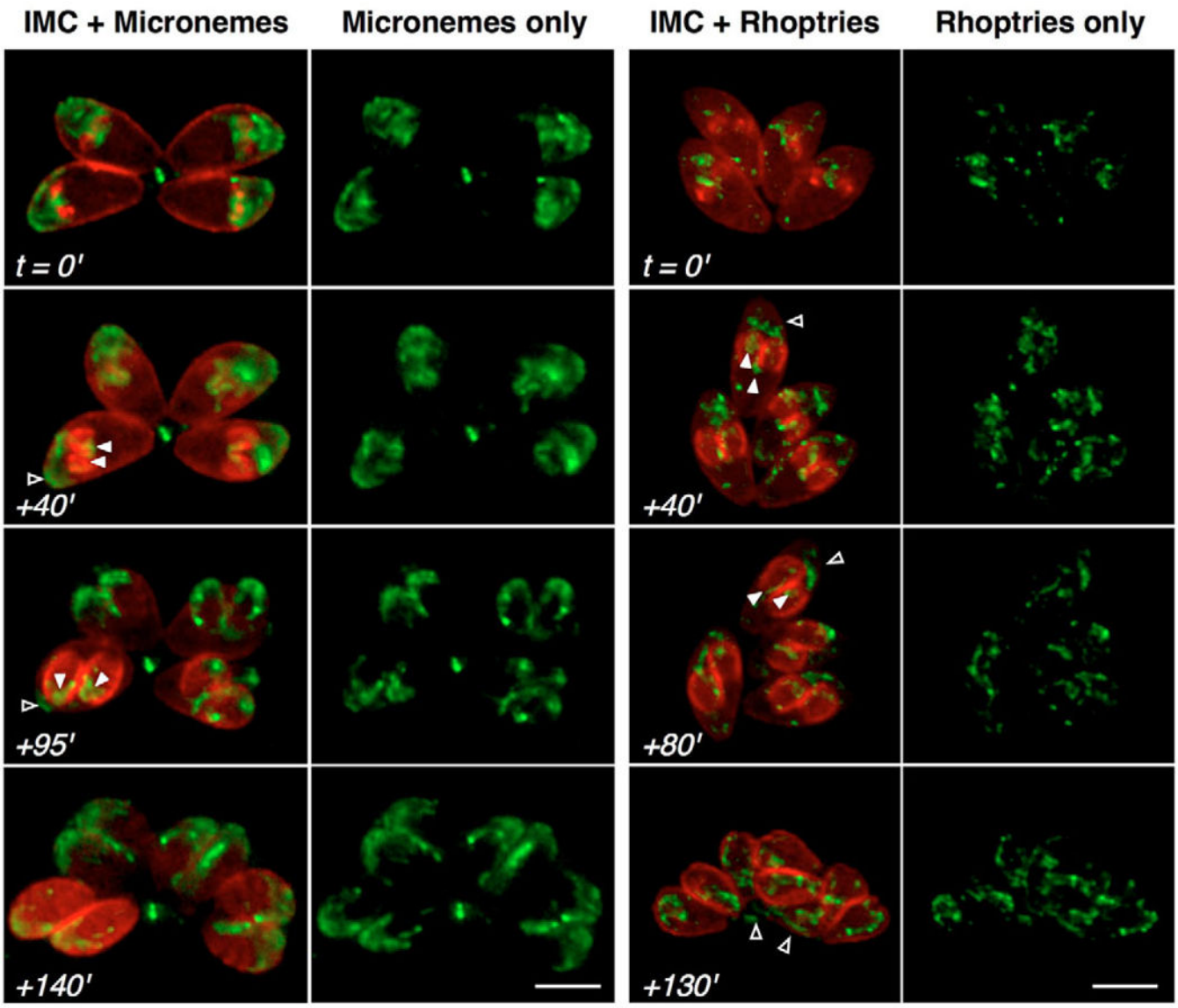

Fig. 4.

Dynamics of microneme and rhoptry biogenesis in *T. gondii.* Parasites expressing MIC3-GFP (left two columns, green) or ROP1-CAT-YFP (right two columns, green) were transfected with IMC1-mRFP (red) in order to track microneme or rhoptry biogenesis. Both organelles are located at the apical end of parasites during interphase (top row). As daughter cells begin to elongate (+40′), new micronemes and rhoptries, distinct from their maternal counterparts, associate with the pellicles of each daughter (white arrowheads). As daughter cells grow, the maternal micronemes and rhoptries (open arrowheads) disappear (+95′ for micronemes, +80′ for rhoptries) and residual material is packaged into residual bodies when daughters emerge (+140′ for micronemes, +130′ for rhoptries). Scale bars: 5 μm.

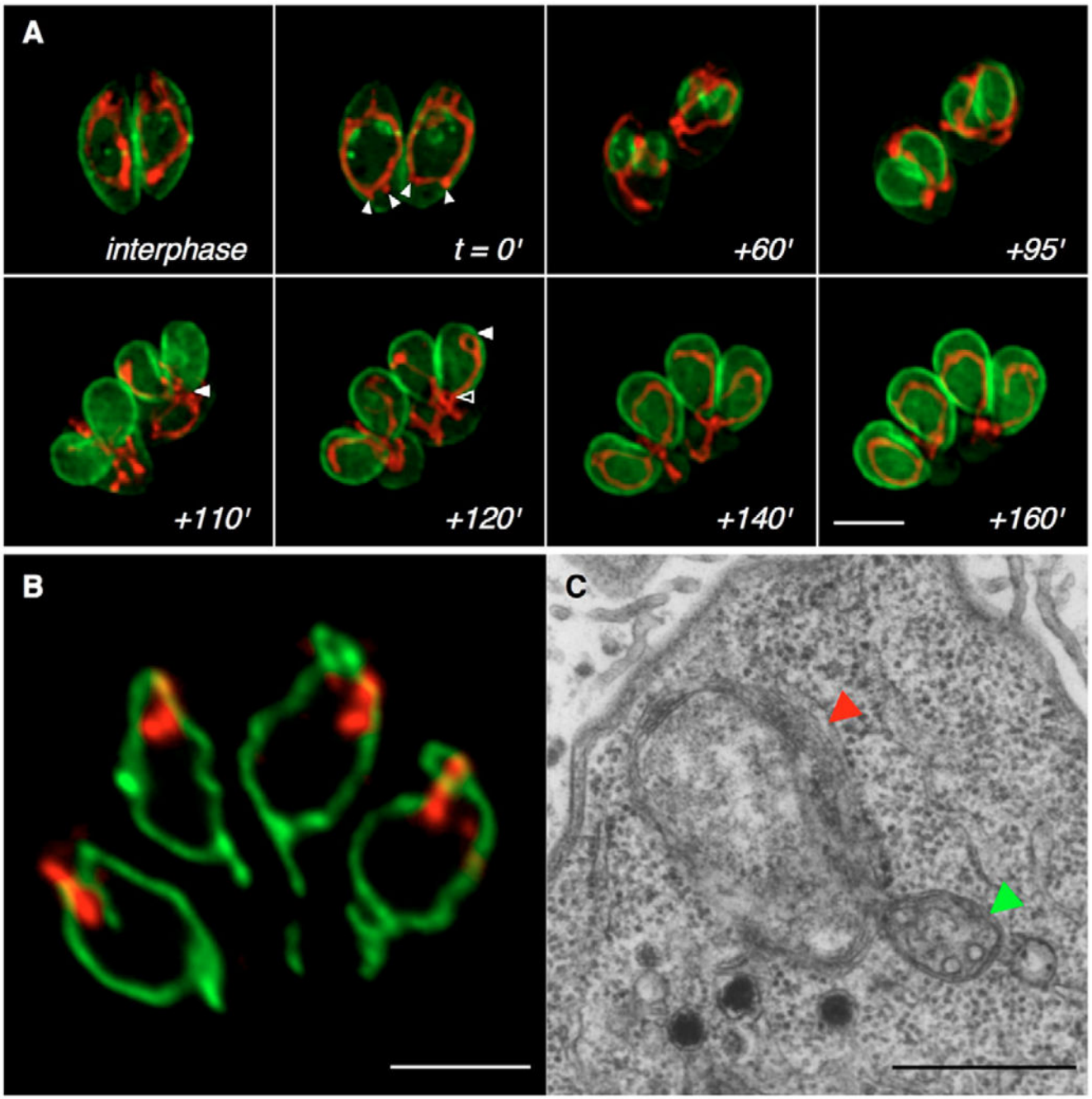

Fig. 5.

Dynamics of mitochondrial replication in *T. gondii.* (A) Time-lapse microscopy of parasites labeled with IMC1-YFP (green) and HSP60-RFP (red). During interphase, the single mitochondrion typically forms an elongated S or lasso shape. The mitochondrion branches at multiple locations during the early stage of daughter IMC formation (arrowheads, t=0′). These branches elongate and often surround the growing daughter IMCs (+60′), but rarely enter into the developing daughters until they begin to emerge from the mother (+110′). Once initiated, however, mitochondrial entry into the daughter cells is very rapid (+120′). A portion of the mitochondrion often remains within the residual material left behind when

daughter parasites emerge after the completion of endodyogeny (+160′). Scale bar: 5 μm. (B) $HSP60_L$-YFP transgenics were fixed and labeled with anti-ACP antibody to reveal transient association of the apicoplast (red) and mitochondrion (green) during the G1 phase and the early stages of apicoplast elongation (before the initiation of daughter scaffold formation). Scale bar: 5 μm. (C) Apicoplast or mitochondrial association is also observed by transmission EM (image kindly provided by G. Warren, University of Vienna, Austria). Scale bar: 0.5 μm.

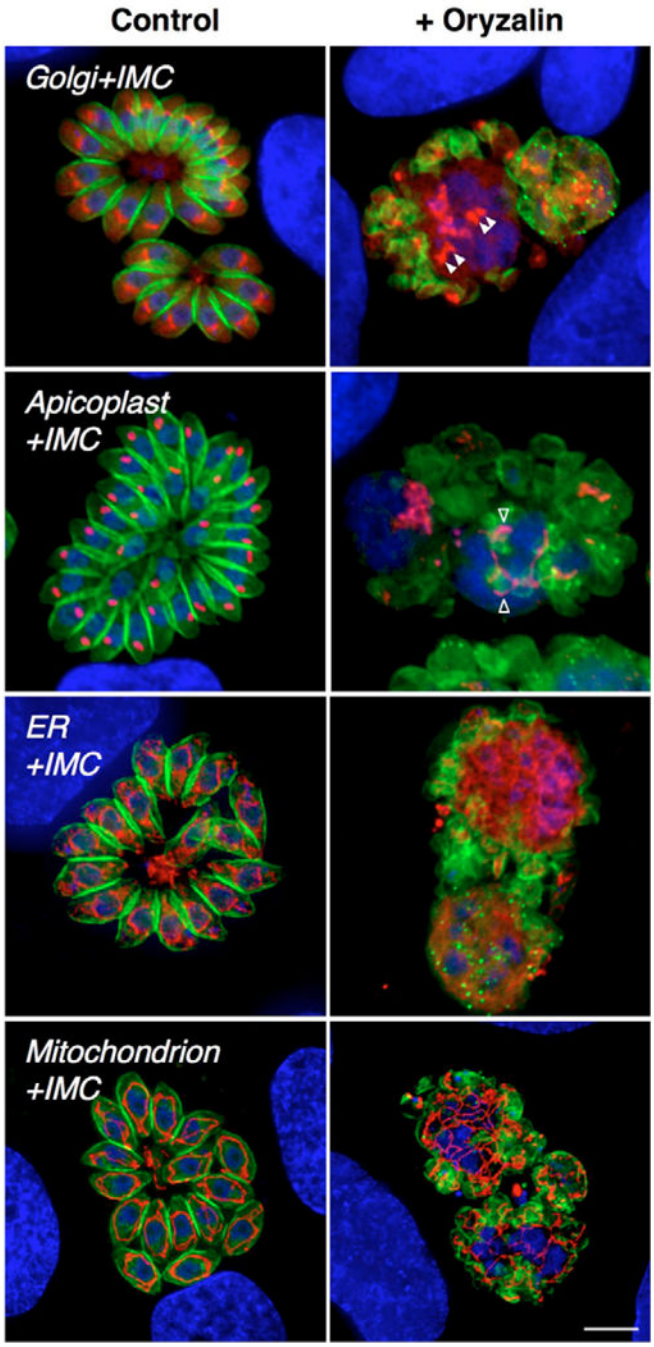

Fig. 6.

Effects of oryzalin on the dynamics of organellar replication. In contrast to control cultures (left), *T. gondii* tachyzoites grown for 24 hours in 1 μM oryzalin (right) fail to organize daughter parasites (green), owing to the absence of subpellicular microtubules (Stokkermans et al., 1996; Morrissette and Sibley, 2002). Early organellar division events, including Golgi division (filled arrowheads), apicoplast elongation (open arrowheads), and ER and mitochondrial ramification still occur in the presence of oryzalin, but later events, such as nuclear, apicoplast, ER and mitochondrial division, do not. In all panels, DNA is labeled

with DAPI (blue) and the inner-membrane complex scaffolding is labeled using IMC1-YFP (green). Red markers: row 1, GRASP-mRFP (Golgi); row 2, anti-ACP (apicoplast); row 3, $P30_L$-mRFP-HDEL (ER); row 4, $HSP60_L$-RFP (mitochondrion). Note the ER and mitochondrial material left behind in the central residual body after the emergence of daughter parasites (bottom two control panels on left). Scale bar: 5 μm.

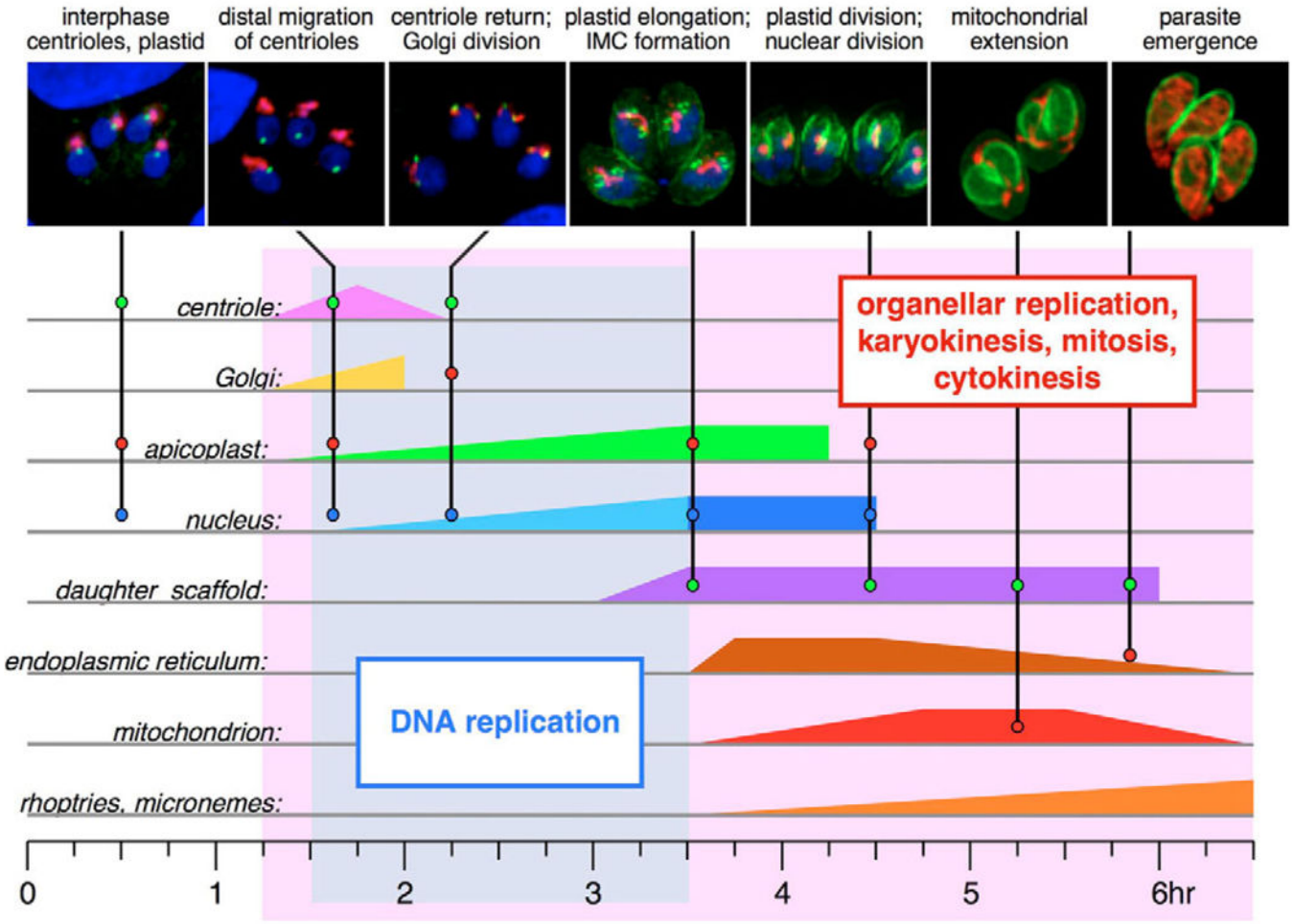

Fig. 7.

Organellar replication: the *T. gondii* cell cycle. The timeline shows the coordination of major events during *T. gondii* tachyzoite cell division (see also Table 1). Morphologically visible events span ~5 hours, representing ~75% of the entire cell cycle [different strains and culture conditions may produce slightly different timing, usually because of differences in the duration of G1 (Fichera et al., 1995; Radke and White, 1998; Radke et al., 2001; Hu et al., 2002; Hu et al., 2004)]. Images show the typical appearance of various organelles during the major morphological transitions associated with their replication (colored circles indicate which organelles are labeled with which color). Data compiled from current studies and previous reports (see Table 1).

Table 1.

Morphological events occurring during replication of *T. gondii* parasite tachyzoites.

Time count (hours:minutes)	Events	Images
0 to 1:15	G1 phase (may vary in length up to 4 hours) *	
	Centriole, Golgi and apicoplast closely associated at the apical end of the nucleus †	Fig. 2A–C
1:15 to 1:45	First morphological changes	
	Centriole migrates away from the apical end ‡	Fig. 2F and Fig. 7 (magenta, increasing)
	Golgi elongates ‡	Fig. 2D and Fig. 7 (yellow, increasing)
	Apicoplast migrates to juxtanuclear region, associates with mitochondrion, and elongates §	Fig. 2E–F, Fig. 5B–C and Fig. 7 (green, increasing)
1:45 to 3:0	Initial stages of mitotic division	
	Centriole divides ‡	Fig. 2I and Fig. 7 (magenta, peak)
	Golgi divides ‡	Fig. 2G and Fig. 7 (yellow, peak)
	Initiation of DNA replication ¶	Fig. 7 (turquoise, increasing)
	Apicoplast continues to elongate §	Fig. 2H–I and Fig. 7 (green, increasing)
	Centriole returns to the apical end and associates with apicoplast ‡	Fig. 2L and Fig. 7 (magenta, decreasing)
3:0 to 3:30	Establishment of the daughter cytoskeleton	
	Daughter conoids form **	Fig. 7 (purple, increasing)
	Spindle poles and intranuclear spindle form **	Fig. 7 (purple, increasing)
	1.8N DNA content ¶	Fig. 7 (turquoise)
	Inner membrane complex assembly begins ††	Fig. 2J–K, Figs 3, 4, Fig. 5A and Fig. 7 (purple)
	Apical ruffling of endoplasmic reticulum ‡‡	Figs 3 and 7 (brown, increasing)
3:30 to 4:30	Organellar partitioning (early stages)	
	Daughter inner membrane complexes elongate ††	Fig. 2M–N, Figs 3, 4, Fig. 5A and Fig. 7 (purple)
	Apicoplast partitioned and divides §	Fig. 2N–O and Fig. 7 (green)
	Nucleus partitioned and divides §§	Fig. 2N–O and Fig. 7 (blue)
	ER partitioned between daughters ‡‡	Figs 3 and 7 (brown)
	Initiation of de novo rhoptry and microneme biogenesis ¶¶	Figs 4 and 7 (orange, increasing)
	Mitochondrion forms branches	Fig. 5A and Fig. 7 (red, increasing)
4:30 to 6:30	Organellar partitioning (late stages)	
	Continued partitioning of ER ‡‡	Figs 3 and 7 (brown, decreasing)
	Continued rhoptry and microneme biogenesis ¶¶	Figs 4 and 7 (orange, increasing)
	Daughter inner membrane complexes complete ††	Figs 3, 4, Fig. 5A and Fig. 7 (purple)
	Mitochondrion enters daughter scaffolds	Fig. 5A and Fig. 7 (red, decreasing)
6:30	Emergence of daughter parasites	
	Daughter parasites bud from mother, picking up plasma membrane ‡‡	Fig. 3 and Fig. 5A

Time count (hours:minutes)	Events	Images
	Residual material left behind (including waste, ER, mitochondrion, plasma membrane etc.)‡‡	Fig. 3, Fig. 5A and Fig. 6

*(Fichera et al., 1995; Radke and White, 1998; Radke et al., 2001; Hu et al., 2002; Hu et al., 2004)

†(Sheffield and Melton, 1968; Bannister et al., 2000a; Striepen et al., 2000; Ferguson et al., 2005; Hartmann et al., 2006)

‡(Hartmann et al., 2006; Pelletier et al., 2002)

§(Striepen et al., 2000)

¶(Radke et al., 2001; Hu et al., 2002; Hu et al., 2004)

**(Hu et al., 2006)

††(Hu et al., 2002; Mann and Beckers, 2001)

‡‡(Hager et al., 1999)

§§(Hu et al., 2002)

¶¶(Carruthers and Sibley, 1997).